NUMERICAL AND EXPERIMENTAL STUDY OF A SANDWICH BEAM SUBJECTED TO A THREE POINTS BENDING TEST

Ana-Maria TĂLÎNGĂ[1], Florin BACIU[2], Anton HADĂR[3,4,5], Gabriel JIGA[6], Marius-Valentin DRĂGOI[7,*], Andrei ANCUȚA[8,*],

This research includes the analysis of the three points bending behavior of a series of 3D printed sandwich beams subsequent to applying a loading rate of 1 mm/min. The study included the determination of the force reactions applied by the support points, for three different honeycomb cores configurations. These configurations had different angles of cell walls inclination, more precisely of 30, 45, and 60 degrees. The purpose of this research is to verify this type of sandwich beam, different than the regular types used in civil buildings, aeronautics or other applications as resistant elements. In this paper the authors presented the design, manufacturing and testing of sandwich beam, that have PLA honeycomb cores and aluminum skins.

Keywords: sandwich beam; 3D printing; honeycombs; numerical analysis;

1. **Introduction**

Composite materials have had the fastest development in the last 50 years [1]. The volume and domains utilization of composite materials products have constantly increased due to their great versatility. This leads to the development of new solutions to obtain products with high quality and to make them more

[1] Engineer, Faculty of Industrial Engineering and Robotics, National University of Science and Technology POLITEHNICA Bucharest, Romania, e-mail: ana_maria.talinga@upb.ro
[2] Associate Professor, Faculty of Industrial Engineering and Robotics, National University of Science and Technology POLITEHNICA Bucharest, Romania, e-mail: florin.baciu@upb.ro
[3] Professor, Faculty of Industrial Engineering and Robotics, National University of Science and Technology POLITEHNICA Bucharest, Romania, e-mail: anton.hadar@upb.ro
[4] Vice-President, Academy of Romanian Scientists, 3 Ilfov Street, Sector 5, 050045 Bucharest, Romania, e-mail: anton.hadar@upb.ro
[5] Corespondent Member, Technical Sciences Academy of Romania, 26 Dacia Boulevard, Sector 1, Bucharest 030167, Romania; anton.hadar@upb.ro
[6] Professor, Faculty of Industrial Engineering and Robotics, National University of Science and Technology POLITEHNICA Bucharest, Romania, e-mail: gabijiga@yahoo.com
[7] Lecturer, Faculty of Industrial Engineering and Robotics, National University of Science and Technology POLITEHNICA Bucharest, Romania, e-mail: marius.dragoi@upb.ro
[8] Engineer, Faculty of Industrial Engineering and Robotics, National University of Science and Technology POLITEHNICA Bucharest, Romania, e-mail: andrei.ancuta2210@upb.ro

attractive for new markets. The aerospace, defense or high-value top industries does not benefit enough from composites. They are now an inexpensive way to achieve high structural performances. The following sections outline the primary market segments of composites, in this paper being used Al-PLA. Additionally, there are several significant applications and products that are consistently introduced yearly, including but not limited to boats, automobiles, heavy transport vehicles, buildings/constructions, corrosion resistant components, aeronautics, and military applications.

Acording to [2], a composite material is an assembly of materials with unique properties. Natural and synthetic materials often operate together. Synthetic composites were introduced to the aircraft sector to regulate and enhance material qualities to meet destination criteria. Carbon fibers offer the assembly a higher stress resistance.

Composite structures, according to [3] can be classified by: composite beams, composite shells, composite plates, and other composite structures (turbine blades, plane wings, etc).

The layers of the sandwich material are made of a robust and resilient material. The core is lightweight and plays a crucial role in separating the two skins and transmitting forces between them. The core is often composed of materials such as honeycomb (aluminum, paper, plastic), foam (polyurethane, polystyrene), or profiles (metal, plastic).

3D printing refers to the technique of depositing successive layers of material to create various shapes. This additive manufacturing technique enables the fabrication of a three-dimensional object with any geometry. Furthermore, 3D printing distinguishes itself from conventional machining techniques that primarily rely on material removal via procedures like cutting, drilling, and casting, among others. Design engineers may rapidly fabricate prototypes using 3D printers. Consequently, the prototype may be rapidly tested and adjusted. By using these innovative technologies, the manufacturing time is considerably reduced, while conventional methods need several weeks to manufacture similar components. As a result, the given time enables for testing several variations of the components in order to promptly identify the required solution [4].

The purpose of this paper is to make a numerical and experimental study on three different configurations of sandwich beams, with 3D printed cores, at different cell walls inclination angles (30°, 45°, and 60°), subjected to three-points bending.

Composite materials have undergone substantial advancements over the last decades, progressing from the initial utilization of glass fibers and basic polymers to the creation of complex structures that integrate various materials to reach exceptional properties such as high strength, low weight, and prolonged durability. This evolution has enabled essential breakthroughs in using sandwich beams made of composites in current industry.

The sandwich type beam must undergo testing for varied requirements depending on its area of use.

The study [5] provides a numerical assessment of a sandwich beam under shear, validating the results with an experimental component and generating graphics through experimental processing for axial displacement thickness, transverse displacement axial location, and axial stress thickness. The authors validate the theoretical results through FEM numerical analysis, demonstrating the advantages of an adaptive sandwich structure, similar with our structure.

The selection of material is an essential factor in determining the durability of a construction. The sandwich construction described in [6] demonstrates a significantly increased resistance, attributed to the presence of an aluminum core and a carbon skin. However, it is important to note that these materials are not environmentally sustainable.

A study in [7] introduces a Nylon sandwich structure with a core with a complex geometry. The structure is subjected to different shear forces, in different regions of the core. Specifically, the first loading is applied to the re-entry cell, while the second loading is applied to the middle of the core.

By adjusting the relative density of the core after its topological optimization, it is feasible to reduce the amount of material used in the production of sandwich beams, as shown in [8].

2. **Materials and methods**

In this section is presented the design, 3D printing, numerical and experimental analysis of of three configurations of sandwich beams subjected to three-points bending.

2.1 **Manufacturing of sandwich beams**

The 3D CAD software CATIA V5 was used to design the sandwich beam, and it has been imported into Ansys Workbench software. The core geometry was designed as a honeycomb and 3D printed (with parameters: printing temperature - 220°C; infill – 100%; infill type – line; print speed – 70 mm/s) at different angles of inclination of the walls, the *α* angle of the walls being 30°, 45°, and 60° as it can be seen in Fig. 1.

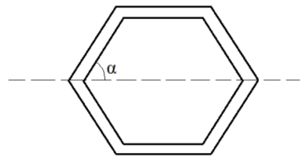

Fig. 1: Inclination angle α of the honeycomb

Using notations from Fig. 2 and measurements specified in Table 1, three types of beam cores have been designed as it can be seen in Fig. 3, 4 and 5, having different angles of inclinations and the aluminium skins.

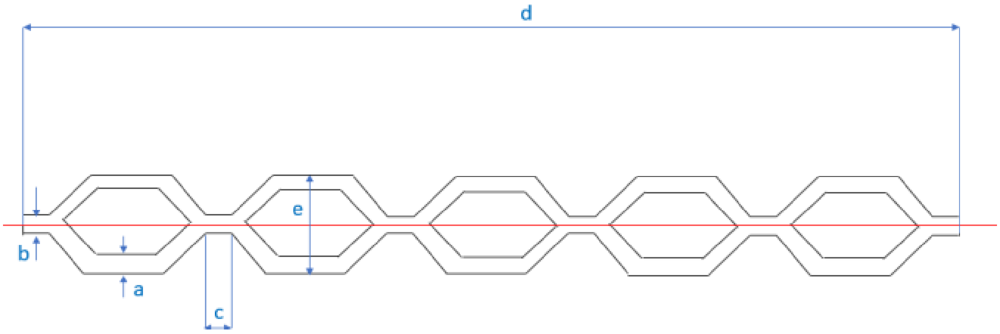

Fig. 2: Honeycombs dimensions notations

Table 1

Dimensions of honeycombs core in millimeters in CATIA V5

a	b	c	d	e	h	t
2.5	5	5	175	16	30	10

Column *h* from Table 1 represents the height of the honeycomb cores whereas column *t* represents the beam thickness.

To generate the sandwich beams, the materials elastic characteristics from Table2 have been considered in the used software.

Table 2

Materials characteristics used in generating sandwich beams

Material	Density [kg/m^3]	Young's modulus [MPa]	Poisson's ratio
Aluminium [9]	2770	70000	0.33
PLA [10]	1400	2131	0.33

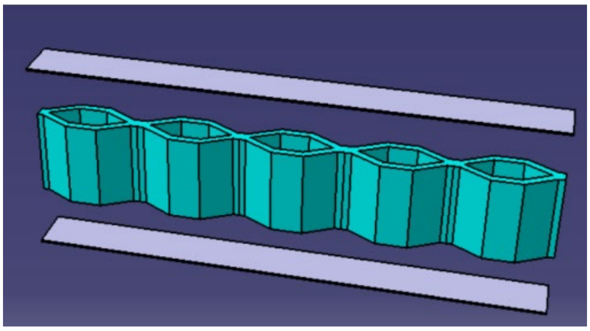
Fig. 3: Geometry of the sandwich beam for the honeycombs with a 30° inclination of the angle

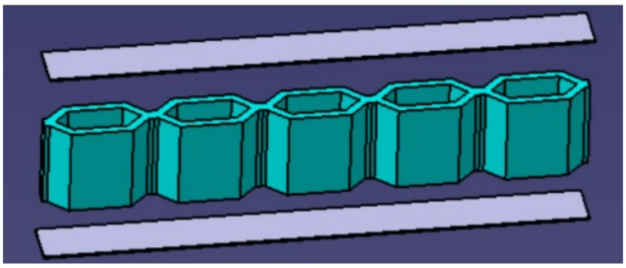

Fig. 4: Geometry of the sandwich beam for the honeycombs with a 45° inclination of the angle

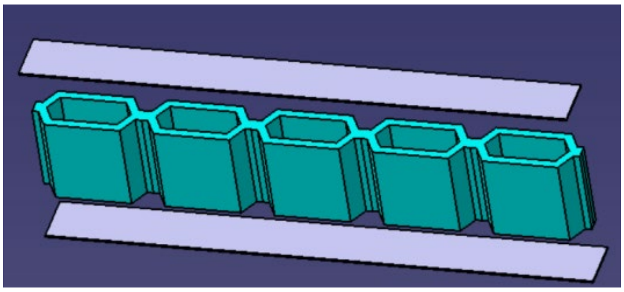

Fig. 5: Geometry of the sandwich beam for the honeycombs with a 60° inclination of the angle

To print the 3D honeycombs, it was used a Vertex 3D printer with software Ultimaker Cura and PLA material, as one can see in Fig. 6. Ultimaker Cura is developed and maintained by Ultimaker B.V., a Dutch company specializing in professional 3D printing solutions. The PLA material is a standard type produced by NatureWorks LLC, United States.

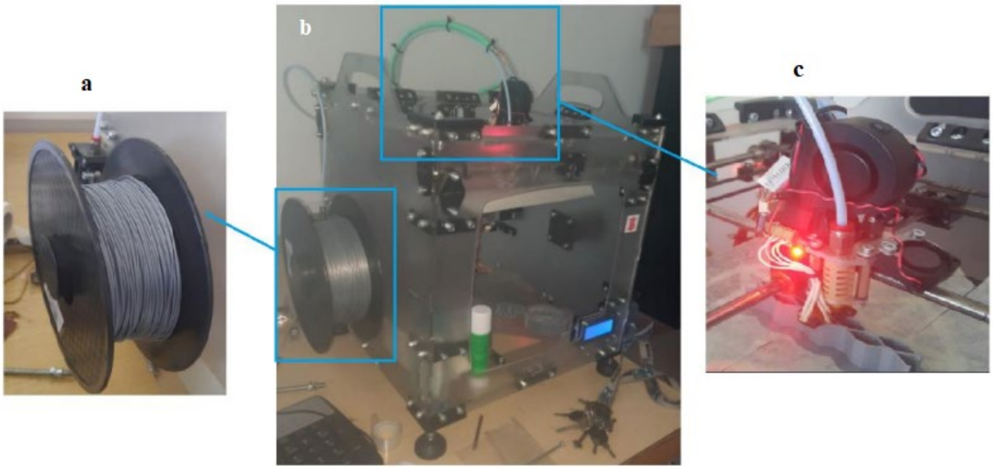

Fig. 6: The 3D printer used: a. PLA filament; b. Printer; c. Printing head.

Fifteen samples were printed, five for each configuration of the honeycomb core. The measurements of each sample can be seen in Tables 3, 4 and 5.

Next notations will be considered:

- F1 - for samples with core walls inclination angle at 30°;
- F2 - for samples with core walls inclination angle at 45°;
- F3 - for samples with core walls inclination angle at 60°.

Table 3

Measurements of the printed samples for core walls angle inclination at 30°

Nr. of sample	**a** [mm]	**b** [mm]	**c** [mm]	**d** [mm]	**e** [mm]	**h** [mm]	**t** [mm]
1	3.43	4.24	4.4	172	16.2	28.55	0.53
2	2.68	4.38	4.57	172	15.71	28.31	0.6
3	2.68	4.38	4.51	172	15.56	28.59	0.51
4	2.45	4.39	4.53	172	15.48	28.85	0.57
5	2.85	4.46	4.22	172	15.97	28.32	0.65
Mean	**2.818**	**4.37**	**4.446**	**172**	**15.784**	**28.524**	**0.572**

Table 4

Measurements of the printed samples for core walls angle inclination at 45°

Nr. of sample	**a** [mm]	**b** [mm]	**c** [mm]	**d** [mm]	**e** [mm]	**h** [mm]	**t** [mm]
1	2.77	4.26	3.2	172	15.81	28.38	0.62
2	3.08	4.35	2.89	172	15.51	28.1	0.54
3	3.15	4.2	3.06	172	16.15	28.67	0.55
4	3.02	4.15	3	172	16.9	28.36	0.6
5	3.01	4.27	2.94	172	15.77	27.61	0.59
Mean	**3.006**	**4.246**	**3.018**	**172**	**16.028**	**28.224**	**0.58**

Table 5

Measurements of the printed samples for core walls angle inclination at 60°

Nr. of sample	**a** [mm]	**b** [mm]	**c** [mm]	**d** [mm]	**e** [mm]	**h** [mm]	**t** [mm]
1	2.53	4.47	3.95	172	15.81	28.14	0.55
2	3	4.36	4.15	172	16.07	28.21	0.6
3	2.89	4.45	4.07	172	15.76	27.35	0.65
4	2.42	4.47	3.96	172	15.4	28.34	0.58
5	3.1	4.42	3.89	172	15.57	28.18	0.73
Mean	**2.788**	**4.434**	**4.004**	**172**	**15.722**	**28.044**	**0.622**

2.2 **Preparation of aluminum skins**

Sandwich beams have PLA honeycombs core and aluminium skins. To assembly the beams, the aluminium plates had to be processed by making grooves on these aluminum alloy plates.

Aluminum is often used in the naval and aviation industries due to its properties. Corrosion resistance is a significant characteristic of this metal, attributed to the creation of a safeguarding oxide layer. It exhibits resistance to the chemical reaction caused by either weak or strong nitric acid.

Once the plates were trimmed to the proper dimensions, their surface was treated to create ridges inclined at a 45° angle. This was performed to enhance adhesion with the PLA core.

Universal adhesives facilitate the formation of a strong bond between the two materials. In order to achieve a satisfactory bond, it is essential that the adhesive establishes uniform contact with the surface of both materials involved. As opposed to mechanical fastening - involving a surface perforation, or welding - involving a meltdown of the materials to be bonded, this procedure is distinct.

The presence of roughness may enhance the overall surface area that is accessible for bonding, hence facilitating the formation of a stronger joint. This approach is emphasized in [11].

The used adhesive to bond plates to honeycombs core is BISON Epoxy Universal.

2.3 **Preparation of PLA core and DIC equipment**

Fig. 7 displays the prepared specimens for testing. The specimens were coated to facilitate evaluation through the digital image correlation (DIC) method (Fig. 8).

In order to to enable the measurement of point displacements, on the specimen surface black paint speckles onto a white background were applied.

Fig. 7 The specimens before testing

The Dantec Q400 system uses two cameras to closely replicate human vision. The angle between the two cameras was established at 60°, and the distance to the specimen is roughly 1 meter to accurately capture the displacement of points on the part during deformation.

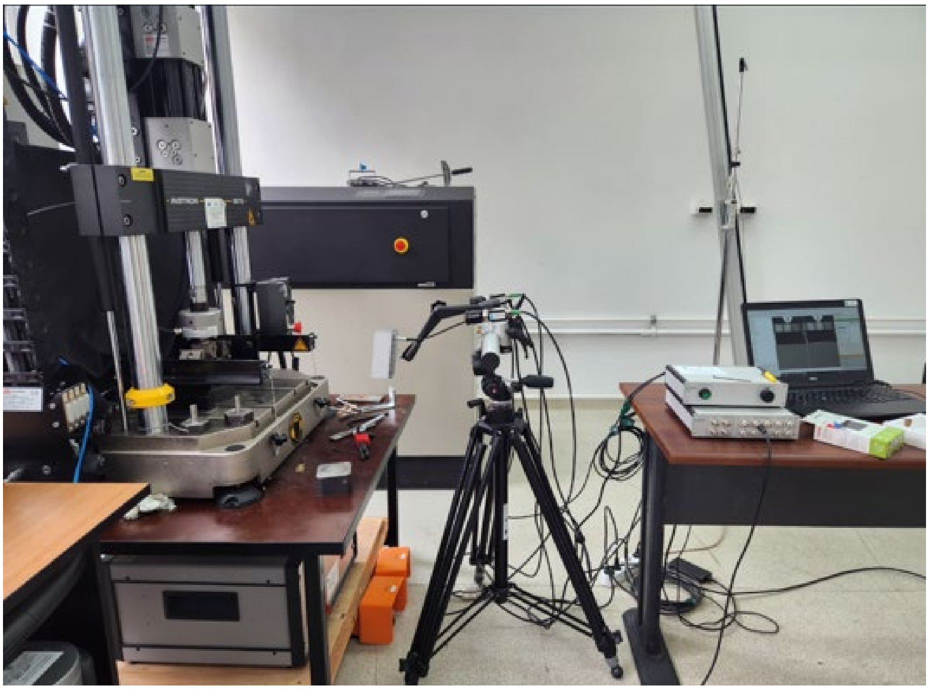

Fig. 8 The equipment used for DIC

Fig. 9 show the sample taken by the camera before starting the three-point bending test, using the digital image correlation (DIC) method.

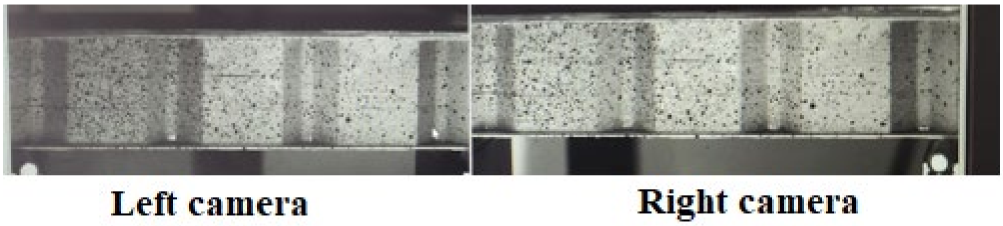

Fig. 9 View of the specimen with the left and the right camera

3. **Results**

3.1 **Experimental results**

The INSTRON 8871 machine (Fig. 10) was used to perform the three-point bending to the sandwich beams.

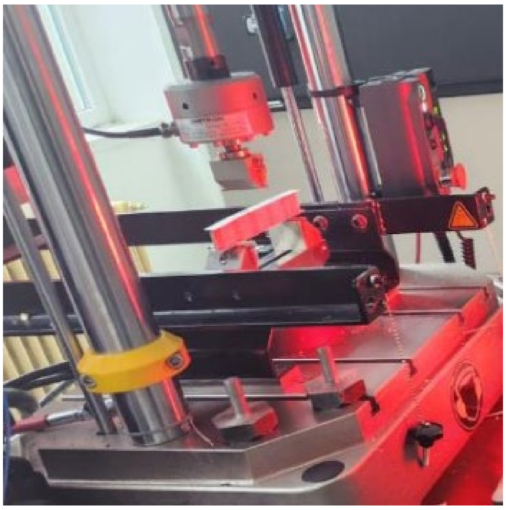

Fig. 10: Positioning of the specimen for a three points bending test

The force levels corresponding to deformations of approximately 0.5 mm were chosen. During the bending test (see Table 6), it is obvious that structure F1, with an inclination angle of 30°, exhibits the greatest strength with respect to the force. The primary cause of the structural failure was largely attributed to adhesive delamination.

Table 6

Centralization of experimentally obtained results

Sample Nr.	F1		F2		F3	
	Force [N]	**Displacement [mm]**	**Force [N]**	**Displacement [mm]**	**Force [N]**	**Displacement [mm]**
1	813.5	0.502	670.3	0.501	861.2	0.501
2	558.5	0.501	642.4	0.506	840.6	0.499
3	547.8	0.505	589.7	0.505	269	0.497
4	932.7	0.504	942.6	0.504	315.8	0.507
5	659.7	0.499	565.9	0.499	568.4	0.501
Average	**702.44**	**0.50282**	**682.18**	**0.50334**	**571**	**0.5014**

3.2 **Numerical study**

Using Ansys Workbench, the sandwich beams components have been generated considering materials dimensions from Table 1 and characteristics from Table 2. Three configurations were meshed using controlled methods to ensure that most elements are hexahedral (see Fig. 11). The F1 configuration resulted in 26070 nodes and 6796 elements, the F2 configuration had 47190 nodes and 8092 elements whereas the F3 configuration had 46762 nodes and 7957 elements.

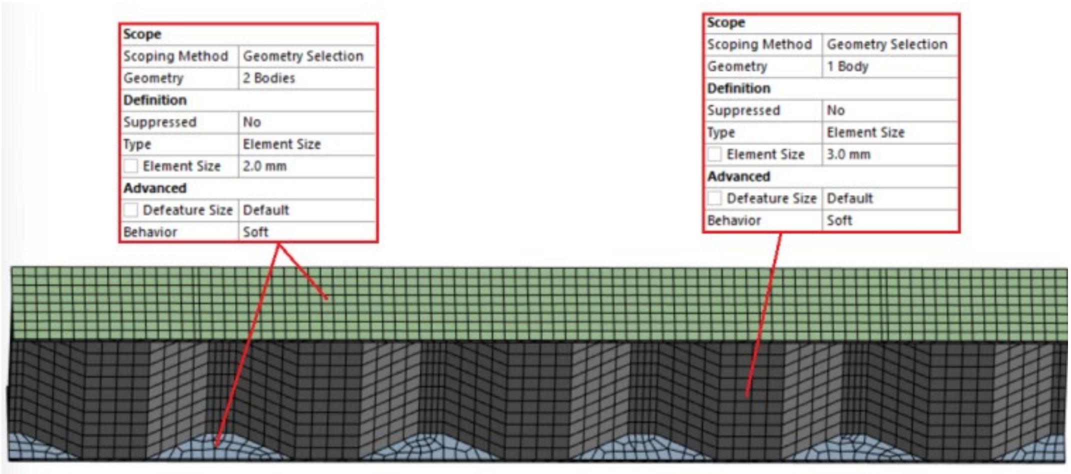

Fig. 11: Structure meshing

The boundary constraints for the three configurations were applied, as could be seen in Fig. 12. The force derived from the experimental test was applied on the top section, while a bearing and joints were used on the bottom section to replicate the experimentally simulated blocking mode.

In the point C, just the Y-axis rotation remained unconstrained, while in the point B, both the X-axis displacement and the Z-axis rotation were left unconstrained (Fig. 12).

C

Type	Remote Displacement
X Component	Free
☐Y Component	0. m (ramped)
☐Z Component	0. m (ramped)
☐Rotation X	0. ° (ramped)
☐Rotation Y	0. ° (ramped)
Rotation Z	Free

A

Type	Force
Define By	Components
Applied By	Surface Effect
Coordinate System	Global Coordintate System
☐X Component	0. N (ramped)
☐Y Component	0. N (ramped)
☐Z Component	702,44 N (ramped)
Suppressed	No

B

Type	Remote Displacement
X Component	Free
☐Y Component	0. m (ramped)
☐Z Component	0. m (ramped)
☐Rotation X	0. ° (ramped)
☐Rotation Y	0. ° (ramped)
Rotation Z	Free

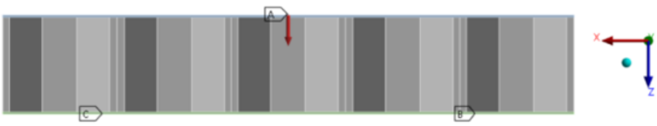

Fig. 12: Constraints and loads application

For the F1 configuration, displacements of around 0.58 mm were observed especially on the aluminum plate. It is clear that the most of the displacements occur near the center of the beam, gradually decreasing towards the edges of the beam (see Fig. 13, 14 and 15).

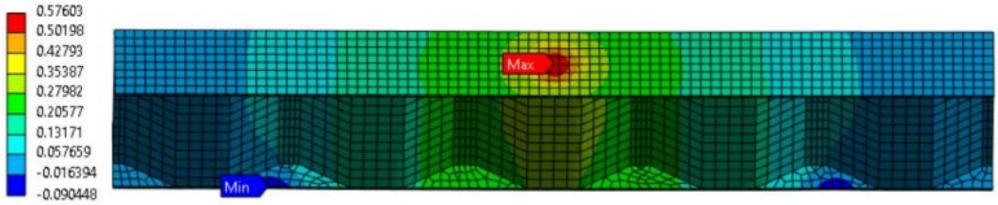

Fig. 13: Deformations along the Z-axis direction for the F1 configuration

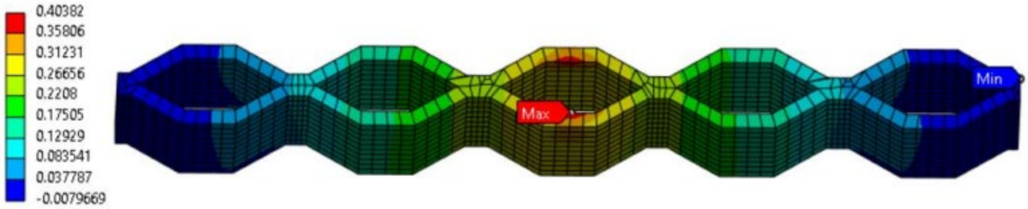

Fig. 14: Deformations in the Z-axis direction in the case of the PLA core for the F1 configuration

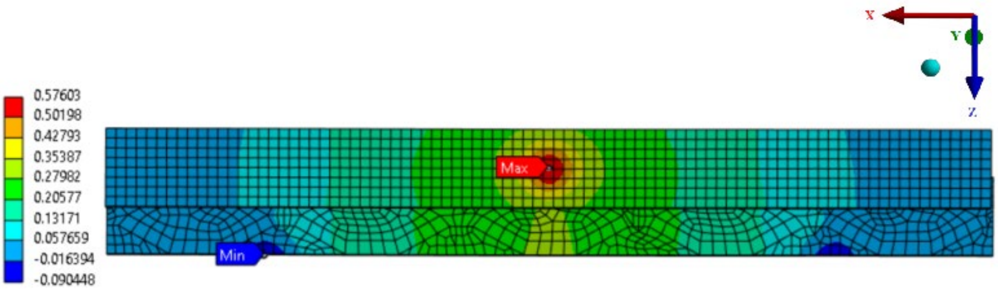

Fig. 15: Deformations in the direction of the Z axis in the case of aluminum for the F1 configuration

For the F2 configuration, deformations of approximately 0.49 mm were observed, this measurement being determined at the middle of the specimen. After undergoing a bending test, the component exhibited symmetrical deformation, with a measured value of approximately -0.04 mm on both sides. The negative values indicates that the component is subjected in compression in certain areas, whereas the positive value indicates the appearance of a stretching (see Fig. 16, 17 and 18).

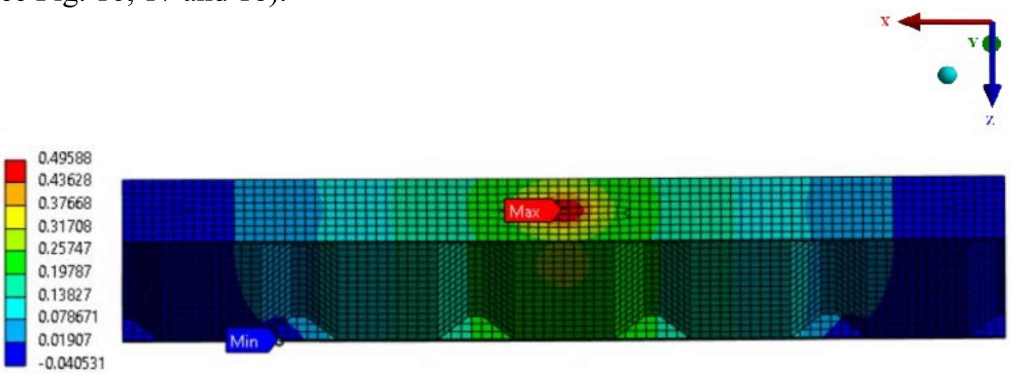

Fig. 16: Deformations along the Z-axis direction for the F2 configuration

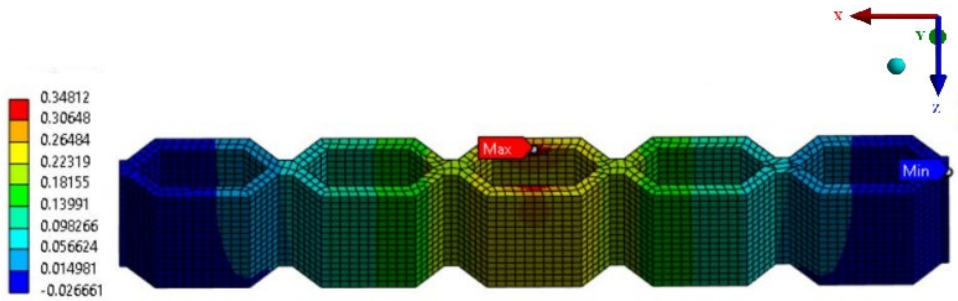

Fig. 17: Deformations in the Z-axis direction in the case of the PLA core for the F2 configuration

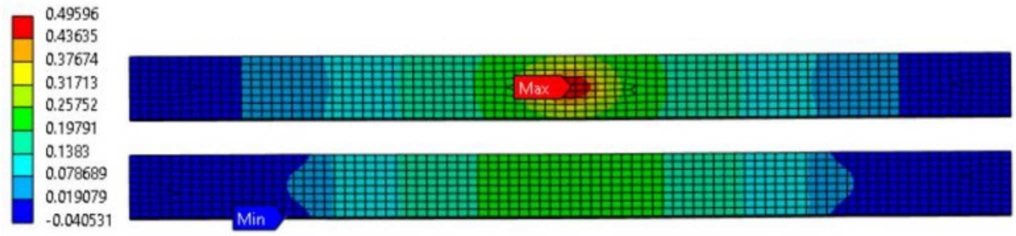

Fig. 18: Total displacements in the case of aluminum for the F2 configuration

For the F3 configuration, deformations of approximately 0.43 mm were observed, this value being observed near the center of the component, similar to the prior configurations (see Fig. 19, 20 and 21).

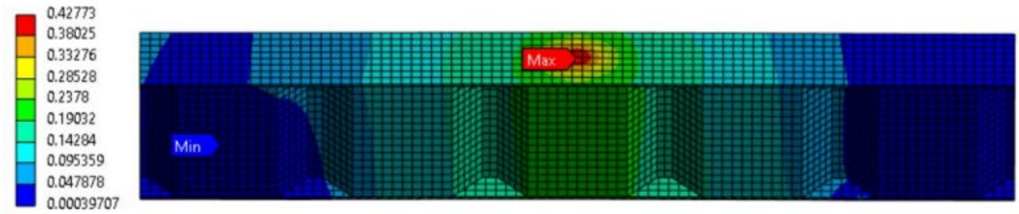

Fig. 19: Total displacements for the F3 configuration

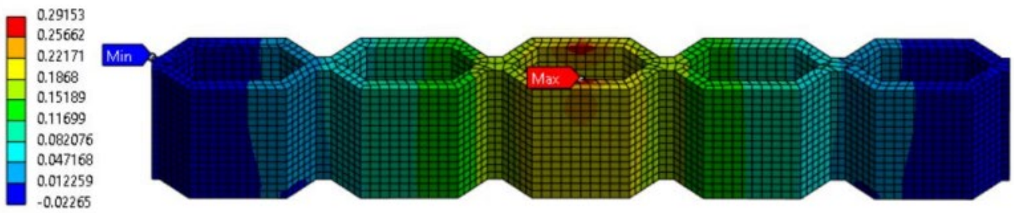

Fig. 20: Total displacements in the case of the PLA core for the F3 configuration

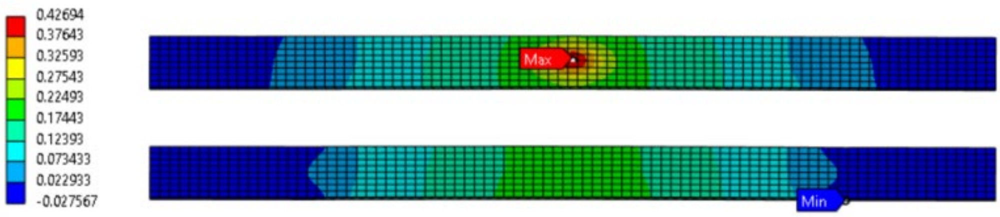

Fig. 21: Total displacements in the case of aluminum for the F3 configuration

From the results obtained, it was observed that aluminum plates are the most loaded. The PLA core took over approximately 32% of total deformation.

4. **Conclusions**

Based on the numerical analysis using FEM (Finite Elements Method), in this paper the authors determined that the sandwich construction with a honeycomb core, inclined at an angle of 30°, provides the greatest resistance. The force value decreases as the angle increases.

The data presented in Table 7 indicates that the deformations of the assembly are exactly the same as the deformations of the aluminum face sheets, for F2 and F3. It may be inferred that the aluminum face sheets take on most of the total deformations. The deformations appeared on the thickness of the aluminum face sheets.

Table 7

Centralization of the obtained results

Configuration	**Structure**	**Total displacements [mm]**	**Reaction force [N]**
F1	Sandwich structure	0.576	702.44
	Aluminium	0.403	
	PLA	0.576	
	Experimental	0.50282	702.44
F2	Sandwich structure	0.496	682.18
	Aluminium	0.496	
	PLA	0.348	
	Experimental	0.50334	682.18
F3	Sandwich structure	0.427	571
	Aluminium	0.427	
	PLA	0.291	
	Experimental	0.5014	571

Upon comparing the experimental results with the numerical ones, acceptable errors below 15% were obtained (see Fig. 22). One initial aspect that leads to these errors is the lack of homogeneity in the core material, exhibiting cavities, cracks, flaws or regions of decreased density. ANSYS is unable to adequately model these particular features.

Errors might also arise as a consequence of the printing process. Due to the contraction and expansion of the material, the dimensions of the parts resulting from 3D printing do not coincide with the specimen dimensions used in the numerical simulation. Consequently, the dimensions of specimens were checked and a mathematical average was computed for various regions. The new data were used to improve the basic geometry in order to closely replicate reality.

The presence of impurities and the preparation procedure of the adhesive can introduce errors. In order to achieve the desired mechanical characteristics of the adhesive, it is essential to use an equal quantity of base and hardener, and ensure that the mixing of these two components is completely uniform, without any presence of air bubbles.

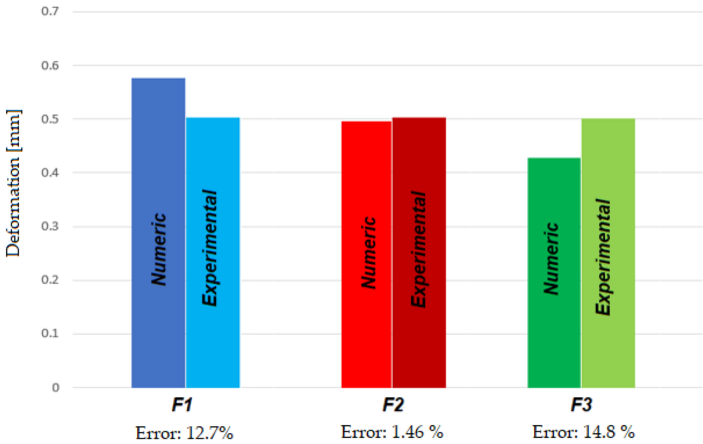

Fig. 22: Experimental and numerical tests comparison

REFERENCES

[1] *S. S. Godara, A. Yadav, B. Goswami, and R. S. Rana*, "Review on history and characterization of polymer composite materials," Mater. Today Proc., vol. 44, pp. 2674–2677, 2021.

[2] *M. Knight, D. Curliss*, "Composite Materials," Encyclopedia of Physical Science and Technology (Third Edition). pp. 455–468, 2003. [Online]. Available: https://www.sciencedirect.com/topics/chemistry/composite-material

[3] *S. Nikbakt, S. Kamarian, and M. Shakeri,* "A review on optimization of composite structures Part I: Laminated composites," Compos. Struct., vol. 195, pp. 158–185, 2018.

[4] *N. Shahrubudin, T. C. Lee, and R. Ramlan*, "An overview on 3D printing technology: Technological, materials, and applications," Procedia Manuf., vol. 35, pp. 1286–1296, 2019.

[5] *X. D. Zhang and C. T. Sun*, "Formulation of an adaptive sandwich beam," Smart Mater. Struct., vol. 5, no. 6, p. 814, 1996.

[6] *I. M. Daniel and J. L. Abot*, "Fabrication, testing and analysis of composite sandwich beams," *Compos. Sci. Technol.*, vol. 60, no. 12–13, pp. 2455–2463, 2000.

[7] *H. Wang, J. Shao, W. Zhang, Z. Yan, Z. Huang, and X. Liang*, "Three-point bending response and energy absorption of novel sandwich beams with combined re-entrant double-arrow auxetic honeycomb cores," Compos. Struct., vol. 326, p. 117606, 2023.

[8] *X. Zhang, C. Xu, W. Li, and Z. Su,* "Study on the bending and shear properties of quasi-honeycomb sandwich structures considering the variable-density core design," *Compos. Struct.*, vol. 324, p. 117517, 2023.

[9] https://www.mit.edu/~6.777/matprops/aluminum.htm (Accessed on 30.06.2025).

[10] *A. Gaweł, S. Kuciel, A. Liber-Kneć & D. Mierzwiński,* "Examination of low-cyclic fatigue tests and poisson's ratio depending on the different infill density of polylactide (PLA) produced by the fused deposition modeling method," Polymers, 15(7), 1651, 2023.

[11] G. *L. Anderson and D. J. Macon,* "Properties of adhesives," in Adhesive Bonding, Elsevier, 2021, pp. 133–155.